

VNN-DERIVED BRAIN AGE GAP PROGRESSION IN INDIVIDUALS AT RISK FOR NEURODEGENERATION

Jason Scheffel[†] Saurabh Sihag[†]

[†] University at Albany, SUNY

ABSTRACT

Neuroimaging is a widely used modality for characterizing neurodegeneration in various health conditions. Brain age gap has emerged as a promising biomarker for monitoring brain health from neuroimaging data using machine learning algorithms. Recent studies have leveraged coVariance neural networks (VNN)-driven pipelines for relatively transparent construction of brain age gap from neuroimaging data. In this paper, we focus on a longitudinal study of VNN-based brain age gap in conjunction with Alzheimer's Progression Score (APS) in individuals that are at a higher risk of neurodegeneration due to family history of Alzheimer's disease. APS is a multimodal marker of disease progression. The longitudinal analysis of APS and VNN-derived brain age gap metrics revealed that a higher risk of disease progression at baseline predicted a larger rate of increase in brain age gap in follow-up visits. Thus, our findings revealed potential stratification in the brain age gap modulated by clinical/biological risks of AD in the at-risk population.

Index Terms— Graph neural networks, covariance, neurodegeneration, biomarkers

1. INTRODUCTION

Aging manifests biologically as various progressive physiological and cognitive changes [22]. Recent years have seen an increased focus in the study of brain aging using machine learning algorithms because of their relevance to digital health and precision medicine [2]. A common objective of brain age prediction strategies is to derive an estimate of brain age from neuroimaging data and compare it with chronological age (time since birth) via the brain age gap, i.e., the difference between brain age and chronological age. A large age gap in the brain has been shown to be indicative of accelerated aging in various neurological diseases, implying a greater burden of the disease and the risk of mortality [18]. Subsequently, we use the notation $\Delta\text{-Age}$ to refer to brain age gap. Prior works have demonstrated that biological changes manifest within the brain at a significant amount of time (months to decades) before the clinical onset of a neurodegenerative condition [34, 4]. Hence, digital markers of brain health, such as $\Delta\text{-Age}$, have the potential to make a significant impact in understanding and detecting neurodegenerative phenomenon in earlier stages of the disease. In this paper, we focus specifically on a cohort with family history of Alzheimer's disease (AD) [36]. Individuals with family history of AD have been reported to be several times more likely to develop AD relative to general population [5].

The main objective of $\Delta\text{-Age}$ prediction in neurodegeneration is to detect or characterize 'accelerated aging' [9, 15]. To this end, a

common template to infer $\Delta\text{-Age}$ consists of: (i) training a regression model to predict chronological age for a healthy population; and then (ii) applying the regression model to predict age for a cohort of interest (often characterized by neurodegenerative condition). A higher $\Delta\text{-Age}$ or its associations with clinical or biological measurements reflective of neurodegeneration hold the most relevance for it to be a biomarker in cohorts with health conditions [20, 12, 28]. Furthermore, existing studies have leveraged longitudinal analysis of $\Delta\text{-Age}$ to demonstrate its association with increasing disease severity in disease populations [14, 10] and mortality risk in healthy individuals [11].

The existing literature in this domain has overwhelmingly focused on achieving near perfect performance in step (i) above with impressive reported accuracies in predicting chronological age across heterogeneous populations of healthy individuals [3, 25, 23]. However, the empirical evidence from several recent studies has hinted that the utility of $\Delta\text{-Age}$ as a biomarker may not necessarily be determined by the prediction accuracy of chronological age on healthy population [3, 17, 28, 26]. Such methodological obscurities in $\Delta\text{-Age}$ add challenges to its interpretation in individuals at risk of neurodegeneration or in the presymptomatic stage as the magnitude of $\Delta\text{-Age}$ alone may not be significantly high or yield information about the underlying pathology. In this context, we leverage the principles of the recently proposed *explanation-driven* pipeline for $\Delta\text{-Age}$ prediction [28, 32] based on VNN models [27] to study $\Delta\text{-Age}$ in at-risk individuals.

1.1. coVariance Neural Networks

VNNs have recently been studied as graph neural networks based on principles of graph signal processing that leverage the sample covariance matrix as the graph shift operator [27, 7, 6, 8, 30, 28]. The convolution mechanism within VNNs takes the form of *linear-shift-and-sum* operators [24] on the covariance matrix. Specifically, given a sample covariance matrix $\mathbf{C} \in \mathbb{R}^{m \times m}$, the convolution operation in a VNN is denoted by a *coVariance filter*, given by $\mathbf{H}(\mathbf{C}) = \sum_{k=0}^K h_k \mathbf{C}^k$, where scalar parameters $\{h_k\}_{k=0}^K$ are the learnable parameters and commonly referred to as filter taps.

VNNs for neuroimaging data analysis. VNNs have shown promise in deriving explainable and anatomically interpretable construction of biomarkers of neurodegeneration in Alzheimer's disease [28, 32, 31, 29]. VNNs offer two key features in the context of deriving biomarkers from neuroimaging data [32]: (i) anatomically interpretable biomarkers [28]; and (ii) cross-validation across neuroimaging datasets curated according to other brain atlases without any re-training [30].

An expanded version of this paper is available at:
<https://sihags.github.io/assets/pdf/ISBI2026.pdf>.

1.2. Contributions

In this paper, we leverage the brain age gap prediction pipeline based on VNNs to study longitudinal evolution of Δ -Age in individuals with family history of AD. The data was part of the PREVENT-AD study [36]. In addition to the structural magnetic resonance imaging (MRI) data, Alzheimer’s Progression score (APS) was also available for each individual. APS is a multimodal metric that has been previously validated as an estimate of disease progression in presymptomatic populations [21]. Our main finding is summarized as follows:

- Baseline neurodegeneration risk, as measured by APS, predicted the trajectory of brain-age gap, with higher initial risk driving faster progression of brain age gap and vice-versa.

The above finding was supported by comprehensive statistical analyses, which further revealed distinct stratifications of at-risk individuals according to rate of progression of brain age gap and baseline APS scores.

Prior works on VNN-driven Δ -Age prediction has focused primarily on neurodegenerative conditions [32, 29, 28, 30, 33]. This paper provides a distinct evaluation than prior works, as it demonstrates the utility of VNN-driven Δ -Age in understanding neurodegenerative patterns in at-risk individuals.

2. METHODS AND MATERIALS

2.1. PREVENT-AD Dataset.

The dataset studied in this paper was a part of the PResymptomatic EValuation of Experimental or Novel Treatments for AD (PREVENT-AD) cohort [36]. The individuals in this dataset were cognitively healthy and identified to be at-risk to developing AD due to parental or multiple-sibling history of AD or related dementias. Such factors put these individuals at an elevated risk of developing AD [5]. For each individual, we used the T1w MRI images from their baseline scan to derive cortical thickness metrics curated according to Destrieux or Desikan-Killiany brain atlases using CAT-12 pipeline [16]. We leveraged the longitudinal structure of the PREVENT-AD dataset to characterize temporal relationships between VNN-derived Δ -Age and APS in at-risk individuals. The longitudinal cohort comprised 703 MRI visits from 343 participants, with follow-up sessions at approximately 3, 12, 24, 36, and 48 months after baseline, yielding visit counts of BL00 ($n = 343$), FU03 ($n = 65$), FU12 ($n = 97$), FU24 ($n = 81$), FU36 ($n = 70$), and FU48 ($n = 47$). Additional demographic details are provided in Appendix A. In total, 103 participants contributed at least two visits suitable for longitudinal modeling. Among these 161 participants, 66 individuals had APS measurements at two or more timepoints (253 total repeated APS measurements), enabling longitudinal modeling of APS trajectories. Per-visit cortical thickness features were processed identically to the cross-sectional analyses (CAT-12 Destrieux parcellation, neuroCombat harmonization, VNN pre-trained on OASIS-3). Longitudinal models indexed time using `time_since_baseline_years`, defined as years elapsed since each participant’s baseline session.

2.2. Δ -Age Prediction.

Preprocessing and Training. The VNN model was trained on the cortical thickness features derived from T1w MRI images collected from 3.0 Tesla MRI scanners for the healthy control population in the publicly available OASIS-3 dataset [19]. The healthy population from OASIS-3 dataset consisted of 598 individuals (age = $68.44 \pm$

7.64 years). The cortical thickness features derived from structural MRIs using Freesurfer 5.3 were available as part of this dataset.

Harmonization was performed using the neuroCombat package [13] on the cortical thickness features to mitigate variance due to different processing pipelines in OASIS-3 and PREVENT-AD datasets. To avoid data leakage between OASIS-3 and PREVENT-AD datasets, we leveraged the cortical thickness features from the CamCAN dataset [35] derived using CAT-12 pipeline [16]. OASIS-3 and PREVENT-AD datasets were harmonized first, and then the harmonization model applied to PREVENT-AD dataset.

VNN was trained to predict the chronological age using the 148 cortical thickness features from the harmonized cortical thickness features of OASIS-3 dataset. The model architecture consisted of 2 hidden layers with width 63 and 14 filter taps in the first hidden layer and width 39 and 22 filter taps in the second hidden layer. ReLU was used as the activation function. This architecture was selected based on a hyperparameter search of 600 trials using the Optuna package [1]. Δ -Age was evaluated according to similar procedure as provided in [28, 32, 33].

3. RESULTS

The longitudinal analysis of the PREVENT-AD dataset helped characterize the temporal relationships between VNN-derived Δ -Age and APS in at-risk individuals. Our preliminary results showed that APS score had an increasing trend over time (approximately 0.083 units per year on average across the considered population), while no such trend was observed for Δ -Age gap. See Appendix C.

3.1. Baseline Values and Future Trajectories

Despite the lack of average change in Δ -Age over time, we examined whether baseline APS and baseline Δ -Age were associated with individual differences in trajectories. We extended the trajectory models to include interactions between time and baseline values, allowing us to test whether individuals with higher baseline scores showed different rates of change over time. For the analysis of baseline APS predicting Δ -Age trajectories, we used the 71 participants who had both baseline APS measurements and longitudinal Δ -Age data, comprising 353 Δ -Age observations across all timepoints for these individuals. We fit the linear mixed-effects model:

$$\begin{aligned} \Delta\text{-Age} \sim & \text{time_since_baseline_years} + \text{baseline_APS} \\ & + \text{time_since_baseline_years} \times \text{baseline_APS} \\ & + \text{APOE4} + \text{time_since_baseline_years} \times \text{APOE4} \\ & + \text{baseline_age} + \text{sex} + \text{baseline_education} \\ & + (1 + \text{time_since_baseline_years})|\text{participant} \end{aligned}$$

Baseline APS was associated with both the level ($\beta = 1.508, p < 0.001$) and the slope ($\text{time} \times \text{baseline APS}: \beta = 0.126, p = 0.013$) of Δ -Age. The level effect replicates the cross-sectional finding that higher APS at baseline is associated with higher Δ -Age. Critically, the significant interaction term indicates that individuals with higher APS at baseline showed faster increases in brain age gap over time. Specifically, for each 1-unit increase in baseline APS, Δ -Age increased by an additional 0.126 years per year of follow-up. This suggests that individuals who already have elevated multimodal markers of preclinical AD at baseline experience accelerated structural brain aging over time.

We then tested the reverse relationship: whether baseline Δ -Age predicted APS trajectories. For this analysis, we used the same 66

participants (253 APS observations) and fit the linear mixed-effects model:

$$\begin{aligned} \text{APS} \sim & \text{time_since_baseline_years} + \text{baseline_}\Delta\text{-Age} \\ & + \text{time_since_baseline_years} \times \text{baseline_}\Delta\text{-Age} \\ & + \text{APOE4} + \text{time_since_baseline_years} \times \text{APOE4} \\ & + \text{baseline_age} + \text{sex} + \text{baseline_education} \\ & + (1 + \text{time_since_baseline_years}|\text{participant}) \end{aligned}$$

Baseline Δ -Age was significantly associated with APS levels ($\beta = 0.111, p = 0.001$), confirming the cross-sectional relationship: individuals with higher brain age gaps at baseline also had higher APS scores throughout the follow-up period. However, baseline Δ -Age was *not* associated with APS slopes (time \times baseline Δ -Age: $\beta = -0.002, p = 0.797$). This null interaction indicates that individuals with higher Δ -Age at baseline did not show faster or slower rates of change in APS over time compared to those with lower baseline Δ -Age.

This asymmetry in the temporal relationships is noteworthy. While baseline APS predicts both the level and rate of change in Δ -Age, baseline Δ -Age predicts only the level of APS but not its rate of change. This pattern suggests a potential temporal ordering in the preclinical disease process: multimodal markers of preclinical AD captured by APS may be upstream of structural brain changes reflected in Δ -Age. In other words, having elevated APS at baseline forecasts how quickly structural brain aging will progress, but having elevated structural brain aging at baseline does not forecast how quickly the broader multimodal disease profile will progress. This could indicate that APS captures pathological processes that drive subsequent structural brain changes, whereas structural brain measures alone may not fully capture the dynamics of multisystem disease progression. Alternatively, this asymmetry could reflect differences in measurement sensitivity: APS, being a composite of multiple modalities, may have greater dynamic range and sensitivity to detect ongoing changes, whereas structural MRI-derived Δ -Age may reach ceiling effects or reflect compensatory mechanisms that obscure direct relationships with future APS progression.

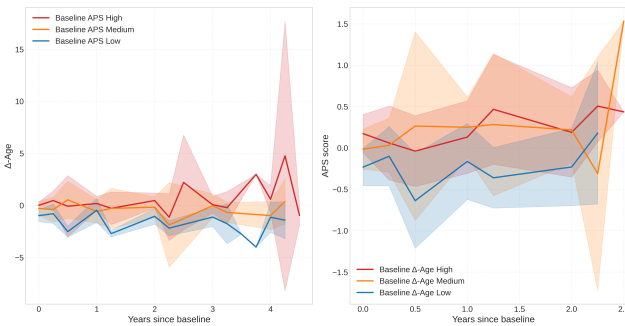


Fig. 1. Asymmetric relationships between baseline values and longitudinal trajectories. **Left panel:** Δ -Age trajectories stratified by baseline APS tertiles (High/Medium/Low). Individuals with higher baseline APS show faster increases in Δ -Age over time (time \times baseline APS: $\beta = 0.126, p = 0.013$). **Right panel:** APS trajectories stratified by baseline Δ -Age tertiles (High/Medium/Low). Baseline Δ -Age was associated with APS levels ($\beta = 0.111, p = 0.001$) but not with APS slopes (time \times baseline Δ -Age: $\beta = -0.002, p = 0.797$).

3.2. Progression Heterogeneity

To characterize heterogeneity in disease progression, we stratified the 66 participants with ≥ 2 APS measurements into tertiles based on their APS slopes (extracted as EBES from the APS trajectory model). The “Fast” progressors ($n = 22$, highest tertile) had mean APS slope = 0.096 units per year, “Medium” progressors ($n = 22$, middle tertile) had mean slope = 0.080 units per year, and “Slow” progressors ($n = 22$, lowest tertile) had mean slope = 0.061 units per year. Baseline characteristics differed substantially across groups. Fast progressors had lower baseline APS (median = -0.957 , range: -1.496 to 0.959) and lower baseline Δ -Age (median = -1.442 , range: -3.539 to 1.163), meaning their brains appeared younger than their chronological age on average. Slow progressors had higher baseline APS (median = 0.764 , range: -0.483 to 2.117) and higher baseline Δ -Age (median = 1.009 , range: -3.606 to 5.672), meaning their brains appeared older than their chronological age. Medium progressors were intermediate on both measures.

Examining Δ -Age trajectories across groups, at baseline (time = 0), Fast progressors had mean Δ -Age = -1.464 years (SE = 0.316 , $n = 23$), Medium progressors had mean = 0.091 years (SE = 0.516 , $n = 22$), and Slow progressors had mean = 0.775 years (SE = 0.520 , $n = 22$). At 2-year follow-up, these differences persisted: Fast progressors had mean Δ -Age = -1.314 years (SE = 0.379 , $n = 17$), Medium progressors had mean = 0.575 years (SE = 0.391 , $n = 15$), and Slow progressors had mean = 1.299 years (SE = 0.689 , $n = 15$). This pattern suggests that progression profiles are fairly stable over this follow-up period, with individuals who start with rapid APS progression (but lower absolute levels) maintaining relatively lower Δ -Age throughout, while those with slower APS progression (but higher absolute levels) maintain relatively higher Δ -Age. This stability may reflect distinct disease trajectories or stages within the preclinical AD spectrum.

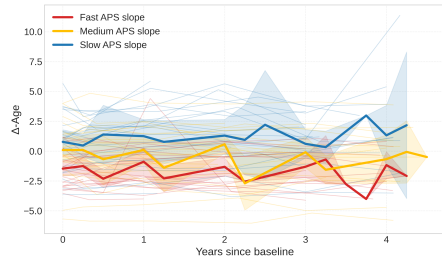


Fig. 2. Individual Δ -Age trajectories stratified by APS progression rate. Participants were divided into tertiles based on their APS slopes (extracted as empirical Bayes estimates): Fast progressors (red, $n = 22$, mean slope = 0.096 units/year), Medium progressors (orange, $n = 22$, mean slope = 0.080 units/year), and Slow progressors (blue, $n = 22$, mean slope = 0.061 units/year). Thin lines represent individual trajectories; thick lines show group means with shaded regions indicating 95% confidence intervals. Fast APS progressors had lower baseline Δ -Age (median = -1.44 years) compared to Slow progressors (median = 1.01 years), suggesting distinct disease trajectories within the preclinical AD spectrum.

To validate the tertile classification, we performed k-means clustering on APS slopes. With $k = 2$ clusters, the algorithm separated individuals into “Low slope” ($n = 29$, mean APS slope = 0.0645) and “High slope” ($n = 37$, mean slope = 0.0885) groups. The Low slope cluster contained all 22 Slow progressors plus 7 Medium

progressors, while the High slope cluster contained all 22 Fast progressors plus 15 Medium progressors. With $k = 3$ clusters, the algorithm produced groups with mean slopes 0.0601, 0.0801, and 0.0962, which aligned almost perfectly with the tertiles: the lowest cluster contained 20/22 Slow progressors, the middle cluster contained 22/22 Medium progressors, and the highest cluster contained 16/22 Fast progressors. This high concordance (overall agreement: $58/66 = 88\%$ for $k = 3$) validates that the progression groups represent distinct data-driven clusters rather than arbitrary divisions, and that the tertile cutpoints correspond to natural separations in the distribution of APS slopes.

Table 1. Clustering validation: alignment between k-means clusters and tertile-based APS progression groups.

(A) k-means with k=2 clusters

k-means Cluster	Slow	Medium	Fast	Total
Low slope (0.065)	22	7	0	29
High slope (0.089)	0	15	22	37
Total	22	22	22	66

Agreement: 44/66 (67%)

(B) k-means with k=3 clusters

k-means Cluster	Slow	Medium	Fast	Total
Low slope (0.060)	20	0	0	20
Medium slope (0.080)	2	22	6	30
High slope (0.096)	0	0	16	16
Total	22	22	22	66

Agreement: 58/66 (88%)

Note: Mean APS slopes (units/year) shown in parentheses. Columns represent tertile-based progression groups; rows represent k-means clusters.

The k=3 solution shows superior concordance (88% vs 67%).

4. DISCUSSION

This longitudinal analysis demonstrates that VNN-derived Δ -Age serves as a dynamic biomarker in individuals at risk for Alzheimer's disease. Baseline APS was associated with both the level and rate of change in Δ -Age (time \times baseline APS: $\beta = 0.126$, $p = 0.013$), whereas baseline Δ -Age was associated with APS levels ($\beta = 0.111$, $p = 0.001$) but not slopes ($p = 0.797$). This asymmetry suggests that APS may capture pathological processes upstream of structural brain changes, with elevated multimodal markers forecasting accelerated structural brain aging. The negative correlation between Δ -Age slopes and APS slopes ($r = -0.433$, $p = 0.0004$) likely reflects different disease stages: individuals with fast APS progression started with lower baseline APS and Δ -Age, potentially representing earlier stages with rapid pathological accumulation, while those with slow APS progression had higher baseline values, potentially approaching plateau phases.

5. REFERENCES

- [1] Akiba, T., Sano, S., Yanase, T., Ohta, T., Koyama, M.: Optuna: A next-generation hyperparameter optimization framework. In: Proceedings of the 25th ACM SIGKDD International Conference on Knowledge Discovery & Data Mining. pp. 2623–2631 (2019)
- [2] Baecker, L., Garcia-Dias, R., Vieira, S., Scarpazza, C., Mechelli, A.: Machine learning for brain age prediction: Introduction to methods and clinical applications. EBioMedicine **72**, 103600 (2021)
- [3] Bashyam, V.M., Erus, G., Doshi, J., Habes, M., Nasrallah, I.M., Truelove-Hill, M., Srinivasan, D., Mamourian, L., Pompilio, R., Fan, Y., et al.: MRI signatures of brain age and disease over the lifespan based on a deep brain network and 14 468 individuals worldwide. Brain **143**(7), 2312–2324 (2020)
- [4] Benussi, A., Alberici, A., Samra, K., Russell, L.L., Greaves, C.V., Bocchetta, M., Ducharme, S., Finger, E., Fumagalli, G., Galimberti, D., et al.: Conceptual framework for the definition of preclinical and prodromal frontotemporal dementia. Alzheimer's & Dementia **18**(7), 1408–1423 (2022)
- [5] Cannon-Albright, L.A., Foster, N.L., Schliep, K., Farnham, J.M., Teerlink, C.C., Kaddas, H., Tschanz, J., Corcoran, C., Kauwe, J.S.: Relative risk for alzheimer disease based on complete family history. Neurology **92**(15), e1745–e1753 (2019)
- [6] Cavallo, A., Gao, Z., Isufi, E.: Sparse covariance neural networks. arXiv:2410.01669 cs.LG (2024), <https://arxiv.org/abs/2410.01669>
- [7] Cavallo, A., Navarro, M., Segarra, S., Isufi, E.: Fair covariance neural networks. arXiv preprint arXiv:2409.08558 (2024)
- [8] Cavallo, A., Sabbaqi, M., Isufi, E.: Spatiotemporal covariance neural networks. In: Joint European Conference on Machine Learning and Knowledge Discovery in Databases. pp. 18–34. Springer (2024)
- [9] Cole, J.H., Franke, K.: Predicting age using neuroimaging: Innovative brain ageing biomarkers. Trends in Neurosciences **40**(12), 681–690 (2017)
- [10] Cole, J.H., Raffel, J., Friede, T., Eshaghi, A., Brownlee, W.J., Chard, D., De Stefano, N., Enzinger, C., Pirpamer, L., Filippi, M., et al.: Longitudinal assessment of multiple sclerosis with the brain-age paradigm. Annals of neurology **88**(1), 93–105 (2020)
- [11] Cole, J.H., Ritchie, S.J., Bastin, M.E., Hernández, V., Muñoz Maniega, S., Royle, N., Corley, J., Pattie, A., Harris, S.E., Zhang, Q., et al.: Brain age predicts mortality. Molecular Psychiatry **23**(5), 1385–1392 (2018)
- [12] Elhaik, E.: Principal component analyses (PCA)-based findings in population genetic studies are highly biased and must be reevaluated. Scientific Reports **12**(1), 1–35 (2022)
- [13] Fortin, J.P., Cullen, N., Sheline, Y.I., Taylor, W.D., Aselcioglu, I., Cook, P.A., Adams, P., Cooper, C., Fava, M., McGrath, P.J., et al.: Harmonization of cortical thickness measurements across scanners and sites. Neuroimage **167**, 104–120 (2018)
- [14] Franke, K., Gaser, C.: Longitudinal changes in individual brainage in healthy aging, mild cognitive impairment, and Alzheimer's disease. GeroPsych: The Journal of Gerontopsychology and Geriatric Psychiatry **25**(4), 235 (2012)
- [15] Franke, K., Gaser, C.: Ten years of brainage as a neuroimaging biomarker of brain aging: What insights have we gained? Frontiers in neurology p. 789 (2019)
- [16] Gaser, C., Dahnke, R., Thompson, P.M., Kurth, F., Luders, E., Alzheimer's Disease Neuroimaging Initiative: CAT—a computational anatomy toolbox for the analysis of structural mri data. biorxiv pp. 2022–06 (2022)

- [17] Jirsaraie, R.J., Gorelik, A.J., Gatavins, M.M., Engemann, D.A., Bogdan, R., Barch, D.M., Sotiras, A.: A systematic review of multimodal brain age studies: Uncovering a divergence between model accuracy and utility. *Patterns* **4**(4) (2023)
- [18] Jové, M., Portero-Otín, M., Naudí, A., Ferrer, I., Pamplona, R.: Metabolomics of human brain aging and age-related neurodegenerative diseases. *Journal of Neuropathology & Experimental Neurology* **73**(7), 640–657 (2014)
- [19] LaMontagne, P.J., Benzinger, T.L., Morris, J.C., Keefe, S., Hornbeck, R., Xiong, C., Grant, E., Hassenstab, J., Moulder, K., Vlassenko, A.G., et al.: OASIS-3: longitudinal neuroimaging, clinical, and cognitive dataset for normal aging and Alzheimer disease. *MedRxiv* (2019)
- [20] Lee, J., Burkett, B.J., Min, H.K., Senjem, M.L., Lundt, E.S., Botha, H., Graff-Radford, J., Barnard, L.R., Gunter, J.L., Schwarz, C.G., et al.: Deep learning-based brain age prediction in normal aging and dementia. *Nature Aging* **2**(5), 412–424 (2022)
- [21] Leoutsakos, J.M., Gross, A., Jones, R., Albert, M., Breitner, J.: ‘Alzheimer’s progression score’: development of a biomarker summary outcome for ad prevention trials. *The journal of prevention of Alzheimer’s disease* **3**(4), 229 (2016)
- [22] López-Otín, C., et al.: The hallmarks of aging. *Cell* **153**(6), 1194–1217 (2013)
- [23] Niu, X., Zhang, F., Kounios, J., Liang, H.: Improved prediction of brain age using multimodal neuroimaging data. *Human brain mapping* **41**(6), 1626–1643 (2020)
- [24] Ortega, A., Frossard, P., Kovačević, J., Moura, J.M., Vandergheynst, P.: Graph signal processing: Overview, challenges, and applications. *Proceedings of the IEEE* **106**(5), 808–828 (2018)
- [25] Peng, H., Gong, W., Beckmann, C.F., Vedaldi, A., Smith, S.M.: Accurate brain age prediction with lightweight deep neural networks. *Medical image analysis* **68**, 101871 (2021)
- [26] Schulz, M.A., Siegel, N.T., Ritter, K.: Brain-age models with lower age prediction accuracy have higher sensitivity for disease detection. *PLoS biology* **23**(10), e3003451 (2025)
- [27] Sihag, S., Mateos, G., McMillan, C., Ribeiro, A.: coVariance neural networks. In: Proc. Conference on Neural Information Processing Systems (Nov 2022)
- [28] Sihag, S., Mateos, G., McMillan, C., Ribeiro, A.: Explainable brain age prediction using covariance neural networks. In: Thirty-seventh Conference on Neural Information Processing Systems (2023), <https://openreview.net/forum?id=cAhJF87GN0>
- [29] Sihag, S., Mateos, G., McMillan, C., Ribeiro, A.: Predicting brain age using transferable coVariance neural networks. In: Proc. IEEE International Conference on Acoustics, Speech, and Signal Processing (Jun 2023)
- [30] Sihag, S., Mateos, G., McMillan, C., Ribeiro, A.: Transferability of covariance neural networks. *IEEE Journal of Selected Topics in Signal Processing* pp. 1–16 (2024). <https://doi.org/10.1109/JSTSP.2024.3378887>
- [31] Sihag, S., Mateos, G., Ribeiro, A.: Towards a foundation model for brain age prediction using covariance neural networks. *arXiv preprint arXiv:2402.07684* (2024)
- [32] Sihag, S., Mateos, G., Ribeiro, A.: Disentangling neurodegeneration with brain age gap prediction models: A graph signal processing perspective. *IEEE Signal Processing Magazine: Special Issue on Accelerating Brain Discovery Through Data Science and Neurotechnology* (2025)
- [33] Sihag, S., Mateos, G., Ribeiro, A.: Explainable brain age gap prediction in neurodegenerative conditions using covariance neural networks. In: *IEEE International Symposium on Biomedical Imaging* (2025)
- [34] Sperling, R.A., Aisen, P.S., Beckett, L.A., Bennett, D.A., Craft, S., Fagan, A.M., Iwatsubo, T., Jack Jr, C.R., Kaye, J., Monteine, T.J., et al.: Toward defining the preclinical stages of alzheimer’s disease: Recommendations from the national institute on aging-alzheimer’s association workgroups on diagnostic guidelines for alzheimer’s disease. *Alzheimer’s & dementia* **7**(3), 280–292 (2011)
- [35] Taylor, J.R., Williams, N., Cusack, R., Auer, T., Shafto, M.A., Dixon, M., Tyler, L.K., Henson, R.N., et al.: The cambridge centre for ageing and neuroscience (cam-can) data repository: Structural and functional mri, meg, and cognitive data from a cross-sectional adult lifespan sample. *neuroimage* **144**, 262–269 (2017)
- [36] Tremblay-Mercier, J., Madjar, C., Das, S., Binette, A.P., Dyke, S.O., Étienne, P., Lafaille-Magnan, M.E., Remz, J., Bellec, P., Collins, D.L., et al.: Open science datasets from PREVENT-AD, a longitudinal cohort of pre-symptomatic Alzheimer’s disease. *NeuroImage: Clinical* **31**, 102733 (2021)

A. DEMOGRAPHICS

The BL00 cohort comprised 343 participants (age 63.62 ± 5.06 years, range 55.17–84.25), including 243 females and 100 males. Participants reported 15.43 ± 3.35 years of education (range 7–29), and 131 individuals carried at least one APOE $\varepsilon 4$ allele. Of these, 103 individuals contributed to the longitudinal imaging subset (those with ≥ 2 MRI visits), with a mean age of 63.89 ± 5.17 years (range 55.25–84.25), 72 females and 31 males, 15.44 ± 3.19 years of education (range 7–24), and 37 $\varepsilon 4$ carriers.

Across all visits, the dataset comprised 703 MRI sessions spanning BL00 (343 visits), FU03 (65), FU12 (97), FU24 (81), FU36 (70), and FU48 (47). The longitudinal imaging subset (participants with ≥ 2 visits) contributed 463 scans (mean 4.50 visits per person, range 2–6), providing observations that extend to FU48 despite APS scores being limited to earlier follow-ups.

APS scores at baseline were available for 161 participants (age 63.66 ± 5.50 years, range 55.17–84.25), comprising 116 females and 45 males with 15.12 ± 3.37 years of education (range 7–29), of whom 62 were APOE $\varepsilon 4$ carriers. Within this group, 66 participants provided longitudinal APS data with measurements at two or more visits (age 63.67 ± 5.75 years, range 55.25–84.25; 46 females, 20 males; 15.53 ± 3.01 years of education, range 9–23; 22 $\varepsilon 4$ carriers). This longitudinal APS cohort contributed 253 measurements across a mean of 3.83 visits per participant (range 2–4), distributed as follows: BL00 (66 visits), FU03 (65), FU12 (63), and FU24 (59). Across all visits with APS measurements, we observed 348 observations from 161 participants, with APS scores ranging from -1.61 to 2.28 (mean 0.02 ± 0.87).

APS scores were available exclusively within the NAP study arm. Of the 162 participants assigned to NAP at BL00, APS values were successfully recorded for 161, whereas PRE participants did not have APS scores. Three individuals (1177880, 3230637, and 6794127) began in NAP at baseline but later transitioned to PRE; consequently, they contribute to the baseline APS counts but lack follow-up APS measurements. These protocol details explain why APS analyses rely on NAP data even though the broader MRI cohort spans both study arms.

B. CROSS-SECTIONAL REPLICATION IN LONGITUDINAL COHORT

Using baseline data from all 343 participants, we replicated the cross-sectional associations via ordinary least squares (OLS) regression. We first fit an OLS model with Δ -Age as the outcome and demographic/genetic covariates as predictors: baseline age, sex, education, and APOE4 carrier status. Age showed a significant negative association with Δ -Age ($\beta = -0.065$, $p = 0.016$), indicating that older individuals at baseline tended to have lower brain age gaps. APOE4 carrier status showed a marginal positive association ($\beta = 0.533$, $p = 0.059$), suggesting APOE4 carriers may have slightly elevated brain age gaps, though this did not reach conventional statistical significance. Sex and education were not significantly associated with Δ -Age.

Among the 161 participants with baseline APS scores, we fit an OLS model to examine the association between Δ -Age and APS while controlling for covariates:

$$\Delta\text{-Age} \sim \text{baseline_APS} + \text{baseline_age} + \text{sex} + \text{baseline_education} +$$

Δ -Age was significantly associated with APS ($\beta = 1.492$, $p < 0.001$), indicating that individuals with higher APS scores at baseline also had higher brain age gaps. This model explained 24.8% of

variance in Δ -Age (adjusted $R^2 = 0.223$). Age showed a strong negative association ($\beta = -0.239$, $p < 0.001$), and sex was also significant ($\beta = -1.197$, $p = 0.006$), with males showing lower Δ -Age. APOE4 carrier status was not significant in this model ($p = 0.535$), suggesting that once APS is accounted for, APOE4 does not independently contribute to explaining Δ -Age. When we extended this model by adding an interaction term (APS \times APOE4), the interaction showed a trend but did not reach statistical significance ($\beta = 0.720$, $p = 0.088$), suggesting that the relationship between APS and Δ -Age may not differ substantially between APOE4 carriers and non-carriers.

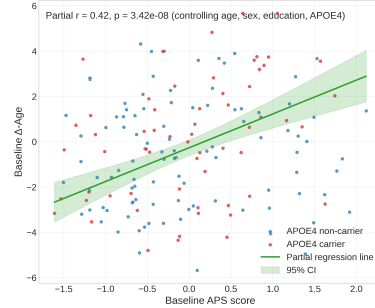


Fig. 3. Baseline cross-sectional association between Δ -Age and APS in the longitudinal cohort ($n = 161$ participants with baseline APS measurements). The partial correlation (controlling for age, sex, education, and APOE4 carrier status) indicates a strong positive relationship. Blue points represent APOE4 non-carriers; red points represent APOE4 carriers. The green line shows the partial regression line with 95% confidence interval (shaded region). Higher baseline APS is associated with higher baseline Δ -Age ($\beta = 1.492$, $p < 0.001$).

C. LONGITUDINAL TRAJECTORIES OF APS AND Δ -AGE

We examined temporal changes in APS and Δ -Age over the follow-up period using linear mixed-effects models with random intercepts and random slopes for time. For APS trajectories, we used the 253 longitudinal APS measurements from the 66 participants who had APS measured at two or more timepoints. We fit the linear mixed-effects model:

$$\begin{aligned} \text{APS} \sim & \text{time_since_baseline_years} + \text{APOE4} \\ & + \text{time_since_baseline_years} \times \text{APOE4} \\ & + \text{baseline_age} + \text{sex} + \text{baseline_education} \\ & + (1 + \text{time_since_baseline_years}|\text{participant}) \end{aligned}$$

APS showed a significant increase over time ($\beta = 0.083$, $p = 0.002$ for the time effect), indicating that APS increases by approximately 0.083 units per year on average. There was no significant main effect of APOE4 ($p = 0.345$) and no time \times APOE4 interaction ($p = 0.767$), indicating that APS trajectories did not differ between APOE4 carriers and non-carriers. Baseline age ($\beta = 0.073$, $p < 0.001$) and male sex ($\beta = 1.081$, $p < 0.001$) were associated with higher APS levels across all timepoints, meaning that older individuals and males tended to have higher APS scores throughout the study period.

For Δ -Age trajectories, we used the 463 longitudinal Δ -Age measurements from all 103 participants who had MRI scans at two

or more timepoints. We fit an analogous linear mixed-effects model:

$$\begin{aligned}\Delta\text{-Age} \sim & \text{time_since_baseline_years} + \text{APOE4} \\ & + \text{time_since_baseline_years} \times \text{APOE4} \\ & + \text{baseline_age} + \text{sex} + \text{baseline_education} \\ & + (1 + \text{time_since_baseline_years}|\text{participant})\end{aligned}$$

In contrast to APS, $\Delta\text{-Age}$ did not show significant change over time in the overall cohort ($\beta = -0.023$, $p = 0.643$ for the time effect). The non-significant negative coefficient suggests a slight numerical decrease in $\Delta\text{-Age}$ over time, but this trend is not statistically distinguishable from zero. There was no significant main effect of APOE4 ($p = 0.411$) and no time \times APOE4 interaction ($p = 0.530$). Baseline age showed a marginal negative association ($\beta = -0.083$, $p = 0.046$), similar to the cross-sectional finding. These results indicate that while APS increases detectably over the follow-up period, global brain age gap ($\Delta\text{-Age}$) does not show a consistent linear increase across all individuals over this relatively short follow-up period (mean follow-up $\approx 2\text{-}3$ years among those with ≥ 2 visits). This difference between APS and $\Delta\text{-Age}$ trajectories suggests that the multimodal composite APS may be more sensitive to detecting short-term changes in preclinical AD progression than structural brain measures alone. However, as demonstrated in subsequent analyses, substantial individual variability exists in $\Delta\text{-Age}$ trajectories that is masked by the population average.

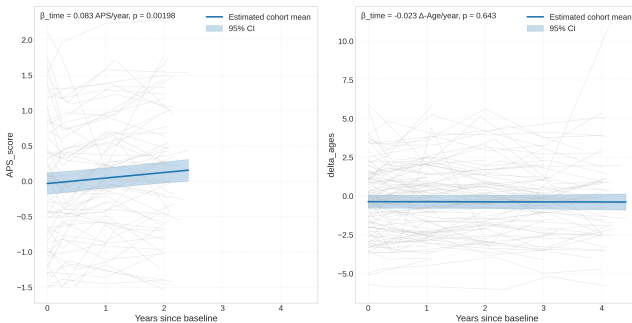


Fig. 4. Longitudinal trajectories of APS and $\Delta\text{-Age}$ over time. **Left panel:** APS shows significant increase over time ($\beta = 0.083$ units/year, $p = 0.002$, $n = 253$ observations from 66 participants). **Right panel:** $\Delta\text{-Age}$ does not show significant change at the population level ($\beta = -0.023$ years/year, $p = 0.643$, $n = 463$ observations from 103 participants). Gray lines represent individual trajectories; blue lines show estimated cohort means with 95% confidence intervals. $\Delta\text{-Age}$.

D. DYNAMICS BETWEEN APS AND $\Delta\text{-AGE}$

To understand how $\Delta\text{-Age}$ and APS co-evolve over time, we extracted individual-level slopes from the mixed-effects trajectory models as empirical Bayes estimates (EBEs). For $\Delta\text{-Age}$ slopes, we extracted EBES from all 103 participants with ≥ 2 MRI visits; for APS slopes, we extracted EBES from the 66 participants with ≥ 2 APS measurements. We then computed partial Pearson's correlations between slopes and baseline values using OLS regression, controlling for baseline age, sex, education, and APOE4 carrier status. The partial correlation between baseline APS and $\Delta\text{-Age}$ slopes was $r = 0.406$ ($p = 0.0006$, $n = 71$), confirming that higher

APS at baseline is associated with steeper $\Delta\text{-Age}$ slopes. Among the 66 participants with both APS and $\Delta\text{-Age}$ slopes, the partial correlation between $\Delta\text{-Age}$ slopes and APS slopes was $r = -0.433$ ($p = 0.0004$). This negative correlation indicates that individuals with faster APS progression showed slower $\Delta\text{-Age}$ progression, and vice versa. This initially counterintuitive finding may reflect different stages within the preclinical disease continuum. Individuals with fast APS progression tended to have lower baseline $\Delta\text{-Age}$ (mean = -1.46 years) and lower baseline APS (mean = -0.96), suggesting they may represent earlier stages of preclinical AD where pathological processes are accumulating rapidly but have not yet manifested as substantial structural brain changes. Conversely, individuals with slow APS progression had higher baseline $\Delta\text{-Age}$ (mean = $+0.78$ years) and higher baseline APS (mean = $+0.76$), potentially reflecting later preclinical stages where both structural and multimodal markers are already elevated and rates of change begin to plateau as individuals approach clinical thresholds.

We then conducted path analyses among growth factors (baseline levels and individual slopes) to decompose associations between baseline values and progression. Because mediator and outcome slopes are estimated over the same interval, these results are interpreted as statistical decompositions rather than causal mediation. Indirect effects were estimated using bootstrap confidence intervals (10,000 iterations). For the indirect path from baseline APS to $\Delta\text{-Age}$ slope via APS slope, we examined whether the association between baseline APS and $\Delta\text{-Age}$ slope operates indirectly through APS slope. The indirect path (baseline APS \rightarrow APS slope \rightarrow $\Delta\text{-Age}$ slope) was significant ($\beta_{\text{indirect}} = 0.247$, 95% CI [0.040, 0.551], $p < 0.05$), whereas the residual direct path from baseline APS to $\Delta\text{-Age}$ slope was not ($\beta_{\text{direct}} = -0.169$, 95% CI [-0.359, 0.020], $p > 0.05$). This pattern indicates an *indirect-only association* among growth factors: higher baseline APS relates to steeper $\Delta\text{-Age}$ progression predominantly through its association with APS progression. All models adjust for baseline age, sex, education, and APOE4.

Complementary indirect path from baseline $\Delta\text{-Age}$ to APS slope via $\Delta\text{-Age}$ slope had both the indirect path (baseline $\Delta\text{-Age}$ \rightarrow $\Delta\text{-Age}$ slope \rightarrow APS slope; $\beta_{\text{indirect}} = -0.0006$, 95% CI [-0.0016, -0.00002], $p < 0.05$) and the residual direct path (baseline $\Delta\text{-Age}$ \rightarrow APS slope; $\beta_{\text{direct}} = -0.0022$, 95% CI [-0.0037, -0.0007], $p < 0.05$) as being significant, indicating *complementary associations* (both indirect and direct components) among growth factors. Covariates were the same as above.

We also tested moderation models to examine whether baseline APS and baseline $\Delta\text{-Age}$ interacted synergistically to predict slopes. We fit OLS models with slopes as outcomes, controlling for baseline age, sex, education, and APOE4. Continuous predictors (baseline APS, baseline $\Delta\text{-Age}$, baseline age, baseline education) were mean-centered before constructing interaction terms. For $\Delta\text{-Age}$ slopes as the outcome, we fit:

$$\begin{aligned}\text{slope}_\Delta\text{-Age} \sim & \text{baseline_APS_centered} \times \text{baseline_}\Delta\text{-Age_centered} \\ & + \text{baseline_age_centered} + \text{sex} \\ & + \text{baseline_education_centered} + \text{APOE4}\end{aligned}$$

The interaction term was not significant ($\beta = 0.0123$, $p = 0.185$), indicating that the effects of baseline APS and baseline $\Delta\text{-Age}$ on future $\Delta\text{-Age}$ slopes are additive rather than synergistic. In other words, having both high APS and high $\Delta\text{-Age}$ at baseline does not produce a multiplicative effect on how quickly $\Delta\text{-Age}$ progresses. Similarly, for APS slopes as the outcome, we fit an analogous model and the interaction was not significant ($\beta = -0.0004$, $p = 0.159$). This absence of moderation effects suggests that baseline APS and

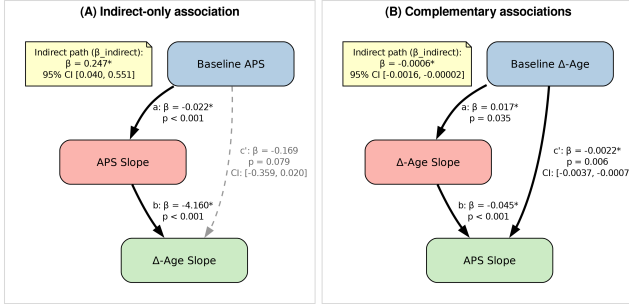


Fig. 5. Path analyses among growth factors linking baseline values and individual slopes. **(A) Indirect-only association:** Baseline APS relates to Δ -Age slopes entirely through APS slopes. The indirect path (Baseline APS \rightarrow APS slope \rightarrow Δ -Age slope) is significant ($\beta_{\text{indirect}} = 0.247$, 95% CI [0.040, 0.551]), whereas the residual direct path is not ($\beta_{\text{direct}} = -0.169$, 95% CI [-0.359, 0.020]). **(B) Complementary associations:** Baseline Δ -Age shows both an indirect path via Δ -Age slopes ($\beta_{\text{indirect}} = -0.0006$, 95% CI [-0.0016, -0.00002]) and a residual direct path to APS slopes ($\beta_{\text{direct}} = -0.0022$, 95% CI [-0.0037, -0.0007]). Analyses adjust for baseline age, sex, education, and APOE4; effects are interpreted as statistical decompositions because mediator and outcome slopes are concurrent. Asterisks (*) indicate $p < 0.05$.

baseline Δ -Age contribute independently to future progression rates, without amplifying or diminishing each other's effects.

E. REGIONAL DYNAMICS

We examined whether the global Δ -Age patterns were reflected at the regional level by fitting linear mixed-effects models for each of the 148 cortical regions. For each region i , we fit two sets of models: one for regional outputs (O_i , the VNN's learned representation of each cortical region at the final layer) and one for regional residuals (r_i , defined as the region-specific difference between the chronological age estimate and the VNN output for that region, which captures the contribution of each region to the overall brain age prediction). Each regional model took the form:

$$\begin{aligned} \text{regional_metric} \sim & \text{time_since_baseline_years} + \text{APOE4} \\ & + \text{time_since_baseline_years} \times \text{APOE4} \\ & + \text{baseline_age} + \text{sex} + \text{baseline_education} \\ & + (1 + \text{time_since_baseline_years})|\text{participant} \end{aligned}$$

Within each of these 148 regional models, both `time_since_baseline_years` and the regional metric (whether O_i or r_i) were z-standardized prior to fitting to stabilize convergence. We applied both Bonferroni correction ($\alpha = 0.05/148 = 0.000338$) and false discovery rate (FDR) correction via the Benjamini-Hochberg procedure to control for multiple comparisons across the 148 regions. For regions showing significant time effects under either correction method, we conducted downstream analyses using OLS regression: (1) testing baseline associations between regional metrics and APS or APOE4 (controlling for baseline age, sex, education), and (2) computing partial Pearson's correlations between regional slopes (extracted as EBEs) and global slopes (Δ -Age slopes and APS slopes), controlling for baseline age, sex, education, and APOE4.

For regional outputs (O_i), 138 of 148 regions (93%) showed statistically significant increases over time after Bonferroni correction, with 146 regions (99%) significant under the more liberal FDR correction. This widespread pattern indicates that the VNN detects structural changes across nearly all cortical regions over the follow-up period. These 138 Bonferroni-significant regions uniformly showed positive baseline associations with APS (138/138 regions, all $p < 0.05$ after Bonferroni correction for 138 tests), meaning that individuals with higher APS scores at baseline had higher regional output values in these regions—the VNN's learned representations of these brain regions already reflected greater pathology at baseline. All 138 regions also showed positive partial correlations with global Δ -Age slopes (138/138 regions, all $p < 0.05$ after Bonferroni correction), meaning that individuals with faster global brain aging also showed faster increases in these regional outputs over time. This consistency between regional and global patterns validates that the VNN's region-specific representations track meaningfully with overall brain aging trajectories.

Regional residuals (r_i) exhibited greater heterogeneity in their temporal patterns. Of 148 regions, 71 showed statistically significant time effects after Bonferroni correction: 46 regions (31%) showed increasing residuals over time while 25 regions (17%) showed decreasing residuals. Under FDR correction, 124 regions showed significant time effects (71 increasing, 53 decreasing). This heterogeneity means that while global brain age increases (as reflected in the positive time effects for outputs), individual regions contribute differently—some regions show residuals that increase over time (meaning these regions increasingly contribute to higher brain age predictions as time progresses, suggesting regional vulnerability) while others show decreasing residuals (meaning these regions contribute less to brain age predictions over time, possibly reflecting relative preservation or compensatory mechanisms). Among the 46 regions with Bonferroni-significant increasing residual trajectories, 45 (98%) showed positive baseline associations with APS ($p < 0.05$ after Bonferroni correction for 46 tests), meaning higher baseline APS was associated with higher residual values in these regions at baseline. All 46 (100%) showed positive partial correlations with global Δ -Age slopes ($p < 0.05$ after Bonferroni correction), confirming that individuals with faster global brain aging also showed faster increases in these regional residuals. Additionally, these regional residual slopes showed negative correlations with global APS slopes (14/46 regions significant at Bonferroni threshold, 45/46 at FDR threshold), reflecting the same inverse relationship seen at the global level: individuals with faster APS progression showed slower increases (or faster decreases) in regional residuals. This consistent pattern across multiple regions validates that the negative slope correlation observed globally is not a statistical artifact but rather a systematic feature that manifests anatomically across cortical regions.

Table 2. Summary of regional dynamics analyses across 148 cortical regions.

Metric	Significant Time Effects	APS Association	Δ -Age Slope Corr.	APS Slope Corr.
<i>Regional Outputs (O_i)</i>				
Bonferroni	138 incr. (93%)	138/138 (100%)	138/138 (100%)	—
FDR	146 incr. (99%)	—	—	—
<i>Regional Residuals (r_i)</i>				
Bonferroni	46 incr., 25 decr.	45/46 (98%)	46/46 (100%)	14/46 (31%)
FDR	71 incr., 53 decr.	—	—	45/46 (98%)

F. ROBUSTNESS CHECKS

As a sensitivity check, we tested for study arm effects on Δ -Age trajectories by fitting a linear mixed-effects model:

$$\begin{aligned} \Delta\text{-Age} \sim & \text{time_since_baseline_years} + \text{study_arm} + \text{APOE4} \\ & + \text{time_since_baseline_years} \times \text{study_arm} \\ & + \text{time_since_baseline_years} \times \text{APOE4} \\ & + \text{time_since_baseline_years} \times \text{study_arm} \times \text{APOE4} \\ & + \text{baseline_age} + \text{sex} + \text{baseline_education} \\ & + (1 + \text{time_since_baseline_years}|\text{participant}) \end{aligned}$$

Consistent with the PREVENT-AD cohort paper indicating these arms could be pooled for analyses, we found no main effect of study arm on Δ -Age ($\beta = -0.068, p = 0.857$), no time \times study arm interaction ($\beta = 0.001, p = 0.996$), and no three-way interaction between time, APOE4, and study arm ($\beta = 0.161, p = 0.432$) [36]. These null findings confirm that the NAP and PRE protocol arms did not differ in their Δ -Age trajectories, validating the appropriateness of pooling them for all analyses. Across all longitudinal models (for both Δ -Age and APS), APOE4 carrier status showed no significant main effects on trajectories or interactions with time (all $p > 0.3$). At baseline, APOE4 showed only a marginal association with Δ -Age ($p = 0.059$) that disappeared when APS was included in the model. This pattern of predominantly null findings for APOE4 suggests that in this at-risk cohort selected specifically for family history of AD, Δ -Age captures risk and progression patterns that are largely independent of APOE4 genotype. This may indicate that family history and APOE4 capture overlapping but distinct dimensions of AD risk, or that in a cohort already enriched for familial risk, APOE4 does not further stratify Δ -Age trajectories.

To assess whether participant dropout biased our longitudinal findings, we compared baseline characteristics between participants retained versus those who dropped out at the FU36 and FU48 visits using Mann-Whitney U tests for continuous variables (age, education, Δ -Age) and chi-squared tests for categorical variables (sex, APOE4 status, study arm). At FU36 (70 retained, 273 dropped out), there were no significant differences in baseline age ($p = 0.228$), education ($p = 0.432$), Δ -Age ($p = 0.770$), sex ($p = 0.789$), or APOE4 status ($p = 0.372$). However, study arm differed significantly ($p < 0.001$), with NAP participants more likely to be retained. This is expected given that APS measurements were only collected in the NAP arm and thus NAP participants had more structured follow-up protocols. At FU48 (47 retained, 296 dropped out), the pattern was similar: no differences in age ($p = 0.118$), education ($p = 0.436$), Δ -Age ($p = 0.788$), sex ($p = 1.000$), or APOE4 ($p = 0.639$), but study arm again differed ($p < 0.001$). These results indicate that attrition was not systematically biased by the key variables of interest (age, Δ -Age, APOE4), and the study arm difference does not affect our conclusions given that we found no study arm effects on outcomes. Participants who dropped out were not systematically different from those retained in ways that would bias the estimated trajectories or associations.